

University of Groningen

IL411 Is a Metabolic Immune Checkpoint that Activates the AHR and Promotes Tumor Progression

Sadik, Ahmed; Somarribas Patterson, Luis F; Öztürk, Selcen; Mohapatra, Soumya R; Panitz, Verena; Secker, Philipp F; Pfänder, Pauline; Loth, Stefanie; Salem, Heba; Prentzell, Mirja Tamara

Published in:
 Cell

DOI:
[10.1016/j.cell.2020.07.038](https://doi.org/10.1016/j.cell.2020.07.038)

IMPORTANT NOTE: You are advised to consult the publisher's version (publisher's PDF) if you wish to cite from it. Please check the document version below.

Document Version
 Publisher's PDF, also known as Version of record

Publication date:
 2020

[Link to publication in University of Groningen/UMCG research database](#)

Citation for published version (APA):

Sadik, A., Somarribas Patterson, L. F., Öztürk, S., Mohapatra, S. R., Panitz, V., Secker, P. F., Pfänder, P., Loth, S., Salem, H., Prentzell, M. T., Berdel, B., Iskar, M., Faessler, E., Reuter, F., Kirst, I., Kalter, V., Foerster, K. I., Jäger, E., Guevara, C. R., ... Opitz, C. A. (2020). IL411 Is a Metabolic Immune Checkpoint that Activates the AHR and Promotes Tumor Progression. *Cell*, 182(5), 1252-1270.e34. <https://doi.org/10.1016/j.cell.2020.07.038>

Copyright

Other than for strictly personal use, it is not permitted to download or to forward/distribute the text or part of it without the consent of the author(s) and/or copyright holder(s), unless the work is under an open content license (like Creative Commons).

The publication may also be distributed here under the terms of Article 25fa of the Dutch Copyright Act, indicated by the "Taverne" license. More information can be found on the University of Groningen website: <https://www.rug.nl/library/open-access/self-archiving-pure/taverne-amendment>.

Take-down policy

If you believe that this document breaches copyright please contact us providing details, and we will remove access to the work immediately and investigate your claim.

Head and Neck IMPT probabilistic dose accumulation: feasibility of a 2 mm setup uncertainty setting

Dirk Wagenaar, Roel G.J. Kierkels, Arjen van der Schaaf, Arturs Meijers, Daniel Scandurra, Nanna M. Sijtsema, Erik W. Korevaar, Roel J.H.M. Steenbakkers, Antje C. Knopf, Johannes A. Langendijk, Stefan Both

PII: S0167-8140(20)30770-2
DOI: <https://doi.org/10.1016/j.radonc.2020.09.001>
Reference: RADION 8502

To appear in: *Radiotherapy and Oncology*

Received Date: 14 February 2020
Revised Date: 14 August 2020
Accepted Date: 2 September 2020

Please cite this article as: Wagenaar, D., Kierkels, R.G.J., van der Schaaf, A., Meijers, A., Scandurra, D., Sijtsema, N.M., Korevaar, E.W., Steenbakkers, R.J.H., Knopf, A.C., Langendijk, J.A., Both, S., Head and Neck IMPT probabilistic dose accumulation: feasibility of a 2 mm setup uncertainty setting, *Radiotherapy and Oncology* (2020), doi: <https://doi.org/10.1016/j.radonc.2020.09.001>

This is a PDF file of an article that has undergone enhancements after acceptance, such as the addition of a cover page and metadata, and formatting for readability, but it is not yet the definitive version of record. This version will undergo additional copyediting, typesetting and review before it is published in its final form, but we are providing this version to give early visibility of the article. Please note that, during the production process, errors may be discovered which could affect the content, and all legal disclaimers that apply to the journal pertain.

© 2020 Published by Elsevier B.V.



1 Head and Neck IMPT probabilistic dose
2 accumulation: feasibility of a 2 mm setup
3 uncertainty setting.

4 **Authors**

- 5 1. Dirk Wagenaar¹ (MSc)
- 6 2. Roel G.J. Kierkels^{1,2} (PhD)
- 7 3. Arjen van der Schaaf¹ (PhD)
- 8 4. Arturs Meijers¹ (MSc)
- 9 5. Daniel Scandurra¹ (MSc)
- 10 6. Nanna M. Sijtsema¹ (PhD)
- 11 7. Erik W. Korevaar¹ (PhD)
- 12 8. Roel J.H.M. Steenbakkers¹ (PhD)
- 13 9. Antje C. Knopf¹ (PhD)
- 14 10. Johannes A. Langendijk¹ (MD/PhD)
- 15 11. Stefan Both¹ (PhD)

16

17 **Affiliations**

- 18 1. Department of Radiation Oncology,
19 University Medical Center Groningen,
20 University of Groningen, The Netherlands
- 21 2. Department of Radiation Oncology,
22 Radiotherapiegroep, Arnhem/Deventer,
23 The Netherlands

24

25 **Corresponding author's details:**

26 Dirk Wagenaar, P.O. Box 30.001, 9700 RB Groningen, the Netherlands
27 ir.d.wagenaar@umcg.nl
28 0652724467

29

30 **Financial disclosure:**

31 Nothing to disclose

32

33 **Running head:**

34 Head and Neck IMPT: a 2 mm setup uncertainty

35 **ABSTRACT**

36 *(MAX. 250 WORDS)*

37 Objective

38 To establish optimal robust optimization uncertainty settings for clinical head and neck cancer (HNC)
39 patients undergoing 3D image-guided pencil beam scanning (PBS) proton therapy.

40 Methods

41 We analyzed ten consecutive HNC patients treated with 70 and 54.25 Gy_{RBE} to the primary and
42 prophylactic clinical target volumes (CTV) respectively using intensity-modulated proton therapy
43 (IMPT). Clinical plans were generated using robust optimization with 5 mm/3% setup/range
44 uncertainties (RayStation v6.1). Additional plans were created for 4, 3, 2 and 1 mm setup and 3%
45 range uncertainty and for 3 mm setup and 3%, 2% and 1% range uncertainty.

46 Systematic and random error distributions were determined for setup and range uncertainties based
47 on our quality assurance program. From these, 25 treatment scenarios were sampled for each plan,
48 each consisting of a systematic setup and range error and daily random setup errors. Fraction doses
49 were calculated on the weekly verification CT closest to the date of treatment as this was considered
50 representative of the daily patient anatomy.

51 Results

52 Plans with a 2 mm/3% setup/range uncertainty setting adequately covered the primary and
53 prophylactic CTV ($V_{95} \geq 99\%$ in 98.8% and 90.8% of the treatment scenarios respectively). The
54 average organ-at-risk dose decreased with 1.1 Gy_{RBE}/mm setup uncertainty reduction and 0.5
55 Gy_{RBE}/1% range uncertainty reduction. Normal tissue complication probabilities decreased by
56 2.0%/mm setup uncertainty reduction and by 0.9%/1% range uncertainty reduction.

57 Conclusion

58 The results of this study indicate that margin reduction below 3 mm/3% is possible but requires a
59 larger cohort to substantiate clinical introduction.

60

61 INTRODUCTION

62 The goal of radiotherapy treatment plan robust optimization is to create a deliverable treatment
63 plan which adequately covers the target volume with the lowest dose possible to the most relevant
64 organs at risk. Treatment preparation and execution uncertainties need to be accounted for to avoid
65 undertreating the target.[1] Composite minimax robust optimization (CMRO) is known to be
66 advantageous for pencil beam scanning (PBS) proton therapy as compared to PTV-based treatment
67 planning which is more sensitive to rigid shifts.[2] Conventionally, the isocentric uncertainty setting
68 used in CMRO is determined by margin recipes for X-ray radiotherapy.[3] For example, van Herk
69 calculated the required CTV-PTV margin to treat the clinical target volume (CTV) to 95% of the
70 prescribed dose for 90% of the patients based on the systematic and random isocentric
71 uncertainty.[1,3] However, the risk of undertreating the target should be weighed against the risk of
72 toxicity to find the optimal uncertainty setting.[4] Furthermore, the van Herk formula assumes dose
73 invariance to external and internal movement which does not hold for proton therapy.[3,5–7]

74 Van der Water et al. studied the effect of setup and range uncertainty setting reduction and found a
75 gradual decrease in normal tissue complication probabilities (NTCPs) as uncertainties were
76 reduced.[4] However, their study did not take anatomical changes or treatment uncertainties into
77 consideration as the target is always covered in the nominal scenario.[4] Changes in anatomy can
78 have a large impact on the delivered dose distribution compared to the planned dose
79 distribution.[8–10] These and other results show that uncertainty setting reduction is impactful on
80 patient-reported toxicities. Previous studies in head and neck cancer (HNC) photon therapy reported
81 toxicity reduction after changing the CTV-planning target volume (PTV) margin from 5 mm to 3 mm,
82 but a further reduction to a 2 mm uncertainty setting might be possible without altering the
83 physician prescribed dosimetric parameters.[11,12] By accumulating the dose on diagnostic quality
84 verification CT images, the impact of interfractional anatomy changes can be evaluated and the
85 delivered dose can be estimated more accurately.[8–10,13] Earlier studies focused on dose
86 accumulation incorporating repeated imaging to study the effect of changing anatomy, but these
87 neglected other treatment uncertainties such as inter- and intrafraction motion which could have a
88 large effect on target coverage.[8,9]

89 In addition to anatomical changes, positional and treatment uncertainties have a large effect on the
90 delivered proton therapy dose distribution in and near the target.[5–7] If the probability density
91 distributions of systematic and random positioning and range errors are known, the probability
92 density distribution of dosimetric parameters can be calculated to predict the tumor control
93 probability (TCP) and normal tissue complication probability (NTCP).[14–16] Such approaches have
94 been extensively studied for probabilistic treatment planning as a way to incorporate
95 uncertainties.[6,17,18] In this study we use a probabilistic approach to retrospectively estimate the
96 dose in different treatment scenarios so that a representative estimation of the actually given dose
97 can be determined.

98 The aim of this study is to establish whether CMRO uncertainty settings can be reduced below 3 mm
99 for HNC IMPT treatments using probabilistic dose accumulation. The probabilistic dose accumulation
100 treatment scenarios incorporating the systematic and random setup and

102 MATERIALS AND METHODS

103 Patients and treatment

104 The study population was composed of the first ten consecutive HNC patients treated with PBS
105 intensity-modulated proton therapy (IMPT) at our institute. Patient characteristics are further
106 described in Table 1. In the Netherlands, patients are selected for proton therapy using model-based
107 selection. In this approach, proton therapy is applied if the Δ NTCP between the proton and photon
108 treatment plans exceeds a certain indication-specific threshold.[14] The Δ NTCP thresholds used for
109 HNC patients are 10% for a single grade II complication, 15% for the combined total of two grade II
110 complications, or 5% for a single grade III complication.[14]

111 Patients were treated with 70 Gy_{RBE} to the primary CTV and 54.25 Gy_{RBE} to the prophylactic CTV in 35
112 fractions with 5 fractions per week using a constant relative biological effectiveness (RBE) factor of
113 1.1. Patients were immobilized using a 5-point mask (HP Pro, Orfit Industries, Wijnegem, Belgium).
114 For each fraction, positioning correction vectors were determined by matching daily cone-beam CT
115 (CBCT) images to the planning CT and applied using a 6-D robotic table capable of yaw, pitch and roll
116 corrections. IMPT treatments were delivered at our proton treatment facility (Proteus[®]Plus, IBA,
117 Ottignies-Louvain-la-Neuve, Belgium). Changes in anatomy were monitored with weekly offline
118 verification CTs (Somatom AS Open, Siemens, München, Germany) with the patient immobilized in
119 treatment position.

120 Treatment planning

121 Clinical treatment plans were generated using CMRO with a 3% range and 5 mm setup uncertainty in
122 the treatment planning system (TPS) (Raystation v6.1, RaySearch Laboratories, Stockholm, Sweden).
123 During optimization, 7 different isocenter shifts (i.e. no shift or a positive or negative shift along one
124 of the three axes) and two (i.e. positive or negative) density shifts are considered. The worst target
125 dose in these 14 scenarios is optimized.

126 Target coverage was assessed using the voxel-wise minimum robustness (multi-scenario) evaluation
127 approach outlined in a recent publication describing the Dutch consensus for proton plan
128 evaluation.[19] During evaluation, 14 different isocenter shifts (i.e. a positive or negative shift along
129 each of the three axes and along each diagonal) and two density shifts were considered resulting in a
130 total of 28 scenario's.[19] The voxel-wise minimum of these 28 scenarios was used to assess robust
131 target coverage, where the coverage criteria was a V_{95} of both CTVs of at least 98%. Eight patients
132 were treated with a four-beam setup with gantry angles between 40-60, 160, 195-200 and 295-320
133 degrees. For one patient, treated for left-sided retromolar trigonum squamous cell carcinoma, the
134 right-sided posterior beam was omitted. Another patient, treated for left-sided tonsillar carcinoma,
135 was treated with unilateral irradiation with three beams angled at 45, 90 and 135 degrees.

136 Treatment plans with various setup and range uncertainty settings are required to conduct this
137 study. These treatment plans with various uncertainty settings were derived from the clinical plan in
138 an automatic process. Therefore in the text we refer to these plans as adjusted treatment plans. The
treatment plans were generated in a two-step process (Figure 1). First the dose distribution
for each setup and range uncertainty is predicted. Second, this predicted dose
is converted into a deliverable adjusted treatment plan using a voxel-based dose

142 mimicking optimization approach. [20,21] This process ensures consistent treatment plan quality in
143 terms of prioritization of the organs at risk to spare, while keeping the physician prescribed tumor
144 coverage unaltered.

145 Additionally, one planner-generated treatment plans per patient was created to validate that the
146 automatic adjustment of treatment plans gives similar results as conventionally created treatment
147 plans. The planner-generated treatment plans were created with a 3 mm setup and 3% range
148 uncertainty. These planner-generated treatment plans were compared to the adjusted treatment
149 plans with a 3 mm setup and 3% range uncertainty in terms of the dose given to at least 98% of the
150 target (D_{98}) in the voxel-wise minimum dose distribution and the dose-fall off outside the CTV in the
151 planned scenario.

152 Using the automated approach, we generated seven adjusted treatment plans per patient with
153 various setup and range uncertainty settings and one planner-generated treatment plan per patient.

154 Error distributions

155 The distributions of the intrafraction shifts were tested for normality by visually inspecting their
156 quantile-quantile (Q-Q) plots and tested for a systematic component using a two-sided Student t-
157 test with an α of 0.05. All other considered error distributions were assumed to be Gaussian. The
158 accuracy of the onboard CBCT imaging system isocenter and 6-D robotic table shifts were assessed
159 based on the results of our comprehensive machine QA program.

160 To estimate the intrafraction isocentric displacement, CBCTs before and after treatment were
161 analyzed. For these patients, CBCTs were made before and after treatment for 41 fractions in total
162 (i.e. 4.1 on average per patient) as part of the post-treatment position verification. The post-fraction
163 CBCTs were matched using rigid registration to estimate the intrafraction isocentric displacement in
164 three dimensions. The distribution of intrafraction displacements was taken as the random setup
165 error distribution and statistically tested for a systematic component. The onboard CBCT and 6-D
166 robotic couch error were quadratically summed and taken as the systematic setup error with an
167 additional 0.5 mm (one standard deviation (SD)) in all directions to account for potentially neglected
168 errors. The magnitude of the residual error was a conservative estimation based on our expectation
169 of unconsidered systematic errors such as intrafraction rotations and methodological uncertainties
170 such as deformable image registration errors.

171 Range errors are systematic in nature and occur depending on tissue type. Common clinical practice
172 is to account for a 2.4% + 1.0 mm range uncertainty error during treatment optimization.[22,23] This
173 recipe was shown to be equal to two SDs in a recent study analyzing the residual range errors in
174 proton radiography validation of our CT calibration curve.[23] The SD of 1.2% + 0.5 mm was
175 converted to a patient-specific percentage by dividing the absolute component by the monitor unit
176 weighted average range of the clinical treatment plan.

177 Probabilistic dose accumulation

178 The error distributions (i.e. CBCT isocenter, robotic table shifts, intrafraction motion, range
179 uncertainty and a residual error) were applied to weekly verification images to simulate the

182 as the accumulated dose of a complete treatment where the random errors have been sampled
183 from their probability density distributions for each fraction.[24] For each treatment plan, 25
184 treatment scenarios were calculated. The workflow of a single treatment scenario calculation is
185 illustrated in figure 2. Seven patients had seven verification CTs and three patients had six
186 verification CTs available. One systematic setup (originating from the CBCT isocenter, robotic table
187 shifts and a residual error) and one systematic range error (originating from proton radiography
188 measurements) were sampled from the error distributions described in the previous subsection.
189 Daily fraction doses were calculated on the weekly verification CT closest to the date of treatment as
190 this was considered to be representative of the patient anatomy of that fraction. In addition to the
191 systematic errors, daily fraction dose calculations included a random setup error (originating from
192 the intrafraction motion). The weekly verification CTs were mapped to the planning CT using a
193 deformable image registration technique previously described by Weistrand et al..[25] Using this,
194 the daily fraction doses were mapped to the planning CT and summed, resulting in an estimated
195 delivered dose distribution for that treatment scenario calculation.

196 The sampled errors were different for each treatment scenario calculation but identical between
197 adjusted treatment plans. A single treatment scenario calculation consisted of 35 fraction dose
198 calculations, each treatment plan was simulated 25 times, each patient had 7 adjusted treatment
199 plans with different uncertainty optimization settings resulting in 61.250 fractional dose calculations
200 in total. Doses were calculated within a 1.0% statistical uncertainty with $3 \times 3 \times 3$ mm³ dose voxels
201 using the Monte Carlo dose engine integrated in the TPS.

202 Statistical analysis

203 In our clinical practice, a target coverage criterion of V_{95} of at least 98% in the voxel-wise minimum
204 dose distribution is applied during treatment. [19] The required coverage of the delivered dose
205 distribution should be more than 98% as the coverage in the voxel-wise minimum dose distribution
206 is less favorable than any single scenario, but less than 100% as this would include clinically
207 irrelevant volumes. When evaluating the delivered dose, a 90% pass-rate is typically accepted since
208 accounting for all possible error scenarios would result in overly large uncertainty settings.[3] In this
209 study, we defined the delivered dose criterion as $V_{95} \geq 99\%$ which should be met for at least 90% of
210 the treated patient population.

211 The target dose was evaluated in terms of the average V_{95} and the fraction of scenarios which met
212 the coverage criteria of $V_{95} \geq 99\%$ for the primary and prophylactic CTVs. Target coverage was
213 further reported in terms of the average tumor control probability (TCP), calculated using a TCP
214 model by Luhr et al..[16] Normal tissue dose was evaluated in terms of the mean dose to OARs and
215 the average NTCP values for xerostomia, grade 2-4 dysphagia, and tube feeding
216 dependence.[14,15]The TCP is calculated based on the DVH in the three regions of the target (i.e.
217 the gross tumor volume (GTV), the primary CTV excluding the GTV and the prophylactic CTV
218 excluding the primary CTV). The sensitivity of the TCP to underdosage of each target region is based
219 on the rate of recurrences in that target region. We chose the other parameters used in the TCP
220 calculation identical to the estimations in the model publication for HNC, which were a tumor
221 control dose D_{50} of 70 Gy_{RBE} and slope γ_{50} of 1.5.[16] The proportion of recurrences was taken from
a model which was based on a study by Due et al who found that the recurrences in
volumes were 82% for the GTV, 16% for the remainder of the primary CTV and
of the prophylactic CTV.[16,26] Due to the low number of recurrences in the

225 prophylactic CTV, the TCP model is less sensitive to underdosage of the prophylactic CTV. An
 226 additional analysis is performed, also using the TCP model by Luhr et al., but using the recurrence
 227 rates of 51.3%, 29.4% and 19.3% for the GTV, the primary CTV and the prophylactic CTV respectively
 228 based on the proportion of recurrences reported to occur in these structures after IMRT in three
 229 centers from a recent study. [27]

230 Insufficient data is available to make an accurate substantiated estimate of D_{50} which has a large
 231 impact on the calculated TCP. Therefore, the calculated TCP does not reflect our clinical results but
 232 can be taken as a relative measure to compare the expected effectiveness of different target dose
 233 distributions. At these settings, a homogenous dose of 70 Gy_{RBE} to the both CTVs yields a TCP of 50%
 234 and a 0.4 Gy_{RBE} dose reduction results in a 1.0% point TCP reduction.

235 The averages of target V_{95} , mean OAR dose, NTCP and TCP were calculated for all patients and
 236 simulations which were then tested for statistical significance by calculating two-tailed p-values
 237 using linear regression analysis (R v3.5.1, R Foundation, Vienna, Austria). The statistical significance
 238 was determined after accounting for multiple testing using Bonferroni's correction.[28] Differences
 239 were considered statistically significant if $p < 0.025$ ($\alpha = 0.05/2$ parameters) for target dose, $p <$
 240 0.0055 ($\alpha = 0.05/11$ parameters) for OAR dose, $p < 0.013$ ($\alpha = 0.05/4$ parameters) for NTCPs and $p <$
 241 0.050 ($\alpha = 0.05/1$ parameter) for TCP.

242 RESULTS

243 The adjusted treatment plans with a 3-mm setup uncertainty created using dose mimicking
 244 optimization resulted in a slightly higher D_{98} of the primary CTV (from 67.0 to 67.1 Gy_{RBE}, $p = 0.82$)
 245 and the prophylactic CTV (from 52.1 to 52.7 Gy_{RBE}, $p = 0.19$) in the voxel-wise minimum dose
 246 distribution compared to the planner-generated treatment plans with identical uncertainty settings
 247 (figure S1). On average, the OAR dose was 0.1 Gy_{RBE} lower for the adjusted treatment plans with
 248 smaller uncertainty settings, but this was not statistically significant ($p = 0.85$) (figure S1).

249 The systematic component of the intrafraction motion derived from the pre and post-treatment
 250 CBCTs was not statistically significant ($p = 0.57, 0.46$ and 0.69 for lateral, longitudinal and height
 251 respectively) (figure S2). The intrafraction motion was therefore considered as random with a 0.7
 252 mm SD in each direction. The error of the onboard CBCT imaging system isocenter and 6-D robotic
 253 couch translation were found to be 0.4 and 0.3 mm (1 SD) respectively. This, together with the 0.5
 254 mm residual error resulted in a 0.7 mm systematic setup error and a 0.7 mm random setup error at
 255 the isocenter (one SD, all directions). The patient-specific range error distribution SD ranged from
 256 1.6% to 1.8%.

257 The results of the treatment scenarios for all adjusted treatment plans are both described below and
 258 shown in table 2.

259 Target coverage and TCP values reduced with smaller setup and range uncertainties (figure 3).
 260 Adjusted treatment plans with a 5, 4, 3 and 2mm setup and 3% range uncertainties met the target
 261 coverage criteria (90% of simulations $V_{95} \geq 99\%$) for both CTVs. When reducing the setup uncertainty
 262 to 1 mm the fraction of simulations meeting the target coverage criteria was
 263 90.8% to 74.8% for the primary CTV and from 90.8% to 70.8% for the prophylactic

264 CTV. The lower dose to the CTVs resulted in a TCP reduction of 0.2%/mm setup uncertainty
 265 ($p=0.013$) and 0.1%/range uncertainty (not significant). Changing the TCP model to use the
 266 recurrence rates found by another study resulted in the same values for TCP reduction as a function
 267 of setup and range uncertainty setting (Figure S3). [27]

268 The average dose to all OARs was reduced linearly by 1.1 Gy_{RBE} /mm setup uncertainty (min = 0.6
 269 Gy_{RBE}/mm, max = 1.4 Gy_{RBE}/mm) and 0.5 Gy_{RBE} /range uncertainty (min = 0.1 Gy_{RBE} /mm, max = 1.3
 270 Gy_{RBE}/mm) (figure 4). The dose differences translated into an NTCP reduction of 1.0%/mm ($p<0.001$),
 271 0.7%/mm ($p<0.001$) and 0.2%/mm ($p<0.001$) setup uncertainty and 0.4%/range (not significant), 0.5%/range
 272 (not significant) and 0.1%/range ($p<0.001$) range uncertainty for xerostomia, grade 2-4 dysphagia and
 273 tube feeding dependence respectively.

274 DISCUSSION

275 In this study, we found a $V_{95} \geq 99\%$ for the primary and prophylactic CTVs for over 90% of the
 276 treatment scenarios for a 2 mm setup uncertainty or larger. We found a small decrease of target
 277 dose which resulted in a TCP reduction of 0.2%/mm setup uncertainty and 0.1%/range
 278 uncertainty. The V_{95} of all adjusted treatment plans was lower for the prophylactic CTV than for the
 279 primary CTV which may be caused by the larger size and anatomical location of the prophylactic CTV,
 280 making its coverage more sensitive to rotations and anatomical changes. As the recurrence rates of
 281 the GTV and primary CTV are higher compared to that of the prophylactic CTV, decreased coverage
 282 of the prophylactic CTV may be clinically less relevant.[16,26] Ideally, reduction of the setup or range
 283 uncertainty setting of the robust optimization is performed by weighing the benefit in toxicity
 284 against the cost in tumor control.

285 In our study, we only found a marginal effect on TCP calculated according to Luhr et al. even when
 286 lowering the setup uncertainty to 1 mm during treatment planning optimization.[16] The TCP is
 287 calculated based on the DVH in the three regions of the target (i.e. the GTV, the primary CTV
 288 excluding the GTV and the prophylactic CTV excluding the primary CTV). The impact of underdosage
 289 of different regions is based on the rate of recurrences in those regions; most recurrences occur in
 290 the GTV. As a result, the TCP model is most sensitive to underdosage of the GTV and therefore, the
 291 TCP is not severely impacted by reducing the setup or range uncertainty as underdosage is most
 292 likely to occur in the GTV-CTV margin and the prophylactic CTV (table 2). The TCP model also
 293 depends on the proportion of recurrences occurring in the different sub-volumes. Therefore we
 294 redid the analysis with the same TCP model but with the proportions of recurrences found in a
 295 recent study, but this change did not impact our results. [27] While the found differences in TCP
 296 were small, the model was calibrated with the conservative assumption that the TCP is 50% for a
 297 homogeneous dose of 70 Gy_{RBE} to the CTV. In practice, the TCP values vary based on patient
 298 characteristics such as p16/HPV positivity which would result in a flatter TCP slope and therefore
 299 even smaller TCP differences.[29]

300 A minor increase in the TCP of the GTV at the last decimal level was observed when the setup
 301 uncertainty decreases from 2mm to 1 mm (Table 2). The magnitude of change is trivial and can be
 302 caused by a random component during Monte Carlo optimization and calculation. Nevertheless, the
 for these setup uncertainty settings and this variation has no impact on our

305 While TCP may be related more directly to local control, DVH parameters are used to assess target
306 coverage in our clinical practice. In our study, we considered a V_{95} of 99% adequate for coverage of
307 the CTV for 90% of the treatment scenarios. However, no clear coverage criterion exists for the
308 actually given dose to the CTV. A V_{95} of 98% is typically aimed for when evaluating the nominal dose
309 to the PTV.[1] However, dose fractionation will cause dose gradients to be less steep (i.e. “blurring”),
310 which washes out some under- and overdosage.[30] Therefore, we chose to apply a 99% coverage as
311 a more stringent criterion to CTV coverage in the estimated actually given dose distribution. If a 98%
312 coverage criteria would have been applied, a setup uncertainty as low as 1 mm would pass for 90%
313 of the treatment scenarios (Figure S4).

314 The average OAR dose decreased by 1.1 $\text{Gy}_{\text{RBE}}/\text{mm}$ setup and 0.5 $\text{Gy}_{\text{RBE}}/\%$ range uncertainty
315 resulting in a summed NTCP reduction of 2.0%/mm setup and 0.9%/range uncertainty. The
316 relation with the range uncertainty setting was not shown to be statistically significant for all tested
317 OARs and NTCP models. The impact on NTCP per 1 mm setup uncertainty reduction was about equal
318 to that of 2% range uncertainty reduction. These results indicate that the setup uncertainty has a
319 higher impact on non-target dose and toxicities than the range uncertainty, indicating the reducing
320 setup uncertainty is of a higher priority than range uncertainty. Currently, we are investigating this
321 further based on daily volumetric imaging and proton radiography for HNC patients treated with PBS
322 in our clinic.

323 The impact of robustness parameters on NTCP values was previously investigated in a planning
324 comparison study in 20 oropharyngeal cases treated with IMPT therapy by van de Water et al.[4]
325 This study found a 0.59%/mm (unilateral) and 1.82%/mm (bilateral) setup uncertainty reduction for
326 dysphagia and a 0.11%/mm (unilateral) and 0.06%/mm (bilateral) range uncertainty reduction for
327 dysphagia. These results are similar to the average dysphagia probability reduction found in this
328 study of 1.0%/mm setup uncertainty and 0.1%/mm range uncertainty. Navran et al. investigated the
329 clinical impact of reducing the CTV-PTV margin retrospectively after reducing their clinical PTV
330 margin for X-ray therapy from 5 mm to 3 mm and found a reduction in the rate of grade 2
331 xerostomia (4.2%), grade ≥ 2 dysphagia (9.4%) and tube feeding dependence (11.4%).[11] These
332 differences are notably higher than the calculated reductions from our study which could be partially
333 explained by the fact that the use of retrospective data does not rule out contributions of other
334 time-dependent factors to the decrease in toxicity.[11] Another influencing factor could be that the
335 patients from the study by Navran et al. were treated with X-ray therapy where the PTV margin may
336 have a larger impact on toxicity due to the larger low and medium dose-bath.[11,31]

337 Our study has some limitations as not all errors could be fully integrated into the treatment scenario
338 calculation. First, the analysis was done entirely on verification CT images but positioning is typically
339 better at the treatment room because of the use of various positioning verification systems leading
340 to an overestimation of the variability in treatment positioning. Second, including more patients
341 would be beneficial as it would include a wider range of anatomical changes but would require a
342 substantial time investment. This was partly alleviated by evaluating multiple treatment scenarios on
343 ten patients, which allowed 250 different treatment scenarios to be calculated. Third, treatment
344 plan adaptations were not taken into consideration and could lead to better target coverage for
345 lower margins as it prevents underdosage by compensating for anatomical changes. Fourth, the
346 was determined only at the isocenter, intrafraction motion may have had a
347 ent if more scans were analyzed per patient, while deformable image registration

348 errors between the planning and verification CTs may have occurred. Lastly, earlier studies showed
349 that the average deformation error is in the order of a millimeter, but this deformation error was
350 present for all adjusted treatment plans and therefore does not bias the results.[25,32]

351 The isocentric intrafraction motion found in our study was normally distributed with a standard
352 deviation of 0.7 mm in each direction. This is relatively small compared to a recent study by Bruijnen
353 et al. investigating the maximum tumor motion using MR in 84 patients who found the 95th
354 percentile of the intrafraction motion to be up to 2.4 mm.[33] In our study, intrafraction motion was
355 only recorded at the isocenter potentially leading to different results. In the study by Bruijnen et al.,
356 larynx patients had the largest intrafraction motion which could also explain the differences in our
357 results as no larynx patients were included in this study.[33]

358 Several measures could improve the treatment accuracy which could further improve these results.
359 A large part of the systematic setup error was the 0.5 mm standard deviation in each direction to
360 account for potentially neglected errors. These errors include delineation errors, registration
361 accuracy and intrafraction deformations. The delineation error was already kept to a minimum as at
362 our institution the target delineation for every patient is evaluated by the entire HNC team which
363 includes not only the HNC radiation oncologists but also a HNC radiologist. In this way, inter-
364 physician delineation variability is accounted for in the target delineation process itself. By improving
365 deformable image registration accuracy and the intrafraction motion assessment, the residual error
366 used in the analysis can be reduced, resulting in smaller shifts and better coverage. Moreover, as
367 more experience is gained, the interfractional motion is expected to decrease due to improved
368 immobilization and treatments are expected to become more robust to motion due to
369 improvements in treatment planning and plan adaptations. Lastly, optimizing patient positioning to
370 minimize the dose perturbation can improve target coverage without increasing the setup
371 uncertainty setting.[34] Future work on estimation of stopping power ratios using dual-energy CT
372 can help reduce the range errors found in proton radiography and reduce the required range
373 uncertainty setting.[23,35] Additionally, future work should be extended to photon therapy where
374 both robust optimization and a probabilistic assessment of target coverage should be used to further
375 improve treatment.[36]

376 This is the first study to incorporate anatomical changes and systematic and random setup and range
377 uncertainties to determine the estimated delivered dose by means of dose mapping and
378 accumulation using longitudinal CT imaging in IMPT HNC patients. All errors were determined for the
379 clinical workflow for the patients under investigation such as intrafraction motion assessments, and
380 the comprehensive machine quality assurance results of the period of treatment. Note that the use
381 of automated adjusted treatment plans is not required for clinical implementation as planner-
382 generated treatment plans were of similar quality. The methodology used in this study offers a more
383 patient outcome driven approach compared to only considering the risk of missing the target as the
384 results of different margins were evaluated in terms of clinically relevant endpoints such as TCP and
385 NTCP.

386 The results of this study indicate a 2 mm/3% setup and range uncertainty is sufficient for optimizing
387 oropharynx HNC robust treatment plans when a 5-point immobilization mask and 6D couch are
used in conjunction with daily CBCT patient alignment. While a larger cohort is needed for

389 clinical adoption, the results indicate that future work will be able to substantiate a 2 mm setup
390 uncertainty setting for HNC IMPT.

391 **ACKNOWLEDGEMENTS**

392 The authors would like to acknowledge Herman Credoe for creating the planner-generated
393 treatment plans to validate the fully automated dose mimicking optimization tool.

394

Journal Pre-proofs

395 **REFERENCES**

- 396 [1] ICRU. ICRU 83 Prescribing, Recording, and Reporting Photon-Beam Intensity-Modulated
397 Radiation Therapy (IMRT). vol. 10. 2010. <https://doi.org/10.1093/jicru/ndq025>.
- 398 [2] Fredriksson A, Bokrantz R. A critical evaluation of worst case optimization methods for robust
399 intensity-modulated proton therapy planning. *Med Phys* 2014;41:081701.
400 <https://doi.org/10.1118/1.4883837>.
- 401 [3] van Herk M, Remeijer P, Rasch C, Lebesque J V. The probability of correct target dosage:
402 dose-population histograms for deriving treatment margins in radiotherapy. *Int J Radiat*
403 *Oncol* 2000;47:1121–35. [https://doi.org/10.1016/S0360-3016\(00\)00518-6](https://doi.org/10.1016/S0360-3016(00)00518-6).
- 404 [4] van de Water S, van Dam I, Schaart DR, Al-Mamgani A, Heijmen BJM, Hoogeman MS. The
405 price of robustness; impact of worst-case optimization on organ-at-risk dose and
406 complication probability in intensity-modulated proton therapy for oropharyngeal cancer
407 patients. *Radiother Oncol* 2016;120:56–62. <https://doi.org/10.1016/j.radonc.2016.04.038>.
- 408 [5] Lomax AJ. Intensity modulated proton therapy and its sensitivity to treatment uncertainties
409 2: the potential effects of inter-fraction and inter-field motions. *Phys Med Biol* 2008;53:1043–
410 56. <https://doi.org/10.1088/0031-9155/53/4/015>.
- 411 [6] Unkelbach J, Bortfeld T, Martin BC, Soukup M. Reducing the sensitivity of IMPT treatment
412 plans to setup errors and range uncertainties via probabilistic treatment planning. *Med Phys*
413 2009;36:149–63. <https://doi.org/10.1118/1.3021139>.
- 414 [7] van der Voort S, van de Water S, Perkó Z, Heijmen B, Lathouwers D, Hoogeman M.
415 Robustness Recipes for Minimax Robust Optimization in Intensity Modulated Proton Therapy
416 for Oropharyngeal Cancer Patients. ` 2016;95:163–70.
417 <https://doi.org/10.1016/j.ijrobp.2016.02.035>.
- 418 [8] Houweling AC, Crama K, Visser J, Fukata K, Rasch CRN, Ohno T, et al. Comparing the
419 dosimetric impact of interfractional anatomical changes in photon, proton and carbon ion
420 radiotherapy for pancreatic cancer patients. *Phys Med Biol* 2017;62:3051–64.
421 <https://doi.org/10.1088/1361-6560/aa6419>.
- 422 [9] Szeto YZ, Witte MG, van Kranen SR, Sonke J-J, Belderbos J, van Herk M. Effects of anatomical
423 changes on pencil beam scanning proton plans in locally advanced NSCLC patients. *Radiother*
424 *Oncol* 2016;120:286–92. <https://doi.org/10.1016/j.radonc.2016.04.002>.
- 425 [10] Meijers A, Jakobi A, Stützer K, Guterres Marmitt G, Both S, Langendijk JA, et al. Log file-based
426 dose reconstruction and accumulation for 4D adaptive pencil beam scanned proton therapy
427 in a clinical treatment planning system: Implementation and proof-of-concept. *Med Phys*
428 2019. <https://doi.org/10.1002/mp.13371>.
- 429 [11] Navran A, Heemsbergen W, Janssen T, Hamming-Vrieze O, Jonker M, Zuur C, et al. The impact
430 of margin reduction on outcome and toxicity in head and neck cancer patients treated with
431 image-guided volumetric modulated arc therapy (VMAT). *Radiother Oncol* 2019;130:25–31.
432 <https://doi.org/10.1016/j.radonc.2018.06.032>.
- 433 [12] Chen AM, Farwell DG, Luu Q, Donald PJ, Perks J, Purdy JA. Evaluation of the Planning Target
434 Volume in the Treatment of Head and Neck Cancer With Intensity-Modulated Radiotherapy:
435 What Is the Appropriate Expansion Margin in the Setting of Daily Image Guidance? *Int J*
436 *Radiat Oncol* 2011;81:943–9. <https://doi.org/10.1016/j.ijrobp.2010.07.017>.

- 439 2010;76:S135-9. <https://doi.org/10.1016/j.ijrobp.2009.06.093>.
- 440 [14] Landelijk Platform Protontherapie, Protontherapie LP. Landelijk Indicatie Protocol
441 Protonen Therapie Hoofd-halstumoren. 2017.
- 442 [15] Wopken K, Bijl HP, van der Schaaf A, van der Laan HP, Chouvalova O, Steenbakkens RJHM, et
443 al. Development of a multivariable normal tissue complication probability (NTCP) model for
444 tube feeding dependence after curative radiotherapy/chemo-radiotherapy in head and neck
445 cancer. *Radiother Oncol* 2014;113:95–101. <https://doi.org/10.1016/j.radonc.2014.09.013>.
- 446 [16] Lühr A, Löck S, Jakobi A, Stützer K, Bandurska-Luque A, Vogelius IR, et al. Modeling tumor
447 control probability for spatially inhomogeneous risk of failure based on clinical outcome data.
448 *Z Med Phys* 2017;27:285–99. <https://doi.org/10.1016/j.zemedi.2017.06.003>.
- 449 [17] Bohoslavsky R, Witte MG, Janssen TM, van Herk M. Probabilistic objective functions for
450 margin-less IMRT planning. *Phys Med Biol* 2013;58:3563–80. <https://doi.org/10.1088/0031-9155/58/11/3563>.
- 452 [18] Bangert M, Hennig P, Oelfke U. Analytical probabilistic modeling for radiation therapy
453 treatment planning. *Phys Med Biol* 2013;58:5401–19. <https://doi.org/10.1088/0031-9155/58/16/5401>.
- 455 [19] Korevaar EW, Habraken SJM, Scandurra D, Kierkels RGJ, Unipan M, Eenink MGC, et al.
456 Practical robustness evaluation in radiotherapy - A photon and proton-proof alternative to
457 PTV-based plan evaluation. *Radiother Oncol* 2019.
458 <https://doi.org/10.1016/j.radonc.2019.08.005>.
- 459 [20] Kierkels RGJ, Fredriksson A, Both S, Langendijk JA, Scandurra D, Korevaar EW. Automated
460 robust proton planning using dose-volume histogram-based mimicking of the photon
461 reference dose and reducing organ at risk dose optimization. *Int J Radiat Oncol Biol Phys*
462 2018;103:251–8. <https://doi.org/10.1016/j.ijrobp.2018.08.023>.
- 463 [21] Fredriksson A. Automated improvement of radiation therapy treatment plans by optimization
464 under reference dose constraints. *Phys Med Biol* 2012;57:7799–811.
465 <https://doi.org/10.1088/0031-9155/57/23/7799>.
- 466 [22] Paganetti H, Niemierko A, Ancukiewicz M, Gerweck LE, Goitein M, Loeffler JS, et al. Relative
467 biological effectiveness (RBE) values for proton beam therapy. *Int J Radiat Oncol*
468 2002;53:407–21. [https://doi.org/10.1016/S0360-3016\(02\)02754-2](https://doi.org/10.1016/S0360-3016(02)02754-2).
- 469 [23] Meijers A, Free J, Wagenaar D, Deffet S, Knopf AC, Langendijk JA, et al. Validation of the
470 proton range accuracy and optimization of CT calibration curves utilizing range probing. *Phys*
471 *Med Biol* 2020;65:03NT02. <https://doi.org/10.1088/1361-6560/ab66e1>.
- 472 [24] Tilly D, Ahnesjö A. Fast dose algorithm for generation of dose coverage probability for
473 robustness analysis of fractionated radiotherapy. *Phys Med Biol* 2015;60:5439–54.
474 <https://doi.org/10.1088/0031-9155/60/14/5439>.
- 475 [25] Weistrand O, Svensson S. The ANACONDA algorithm for deformable image registration in
476 radiotherapy. *Med Phys* 2015;42:40–53. <https://doi.org/10.1118/1.4894702>.
- 477 [26] Due AK, Vogelius IR, Aznar MC, Bentzen SM, Berthelsen AK, Korreman SS, et al. Recurrences
478 after intensity modulated radiotherapy for head and neck squamous cell carcinoma more
479 likely to originate from regions with high baseline [18F]-FDG uptake. *Radiother Oncol*
480 2014;111:360–5. <https://doi.org/10.1016/j.radonc.2014.06.001>.
- 481 [27] Zukauskaite R, Hansen CR, Grau C, Samsøe E, Johansen J, Petersen JBB, et al. Local
after curative IMRT for HNSCC: Effect of different GTV to high-dose CTV margins.
Radiother Oncol 2018;126:48–55. <https://doi.org/10.1016/j.radonc.2017.11.024>.

- 484 [28] Bonferroni CE. Statistical theory of classes and probability calculus. *Publ R High Inst Econ*
485 *Commer Sci Florence* 1936;8:3–62.
- 486 [29] Psyrrri A, Rampias T, Vermorken JB. The current and future impact of human papillomavirus
487 on treatment of squamous cell carcinoma of the head and neck. *Ann Oncol* 2014;25:2101–15.
488 <https://doi.org/10.1093/annonc/mdu265>.
- 489 [30] van Herk M, Witte M, van der Geer J, Schneider C, Lebesque J V. Biologic and physical
490 fractionation effects of random geometric errors. *Int J Radiat Oncol Biol Phys* 2003;57:1460–
491 71. <https://doi.org/10.1016/j.ijrobp.2003.08.026>.
- 492 [31] Arts T, Breedveld S, de Jong MA, Astreinidou E, Tans L, Keskin-Cambay F, et al. The impact of
493 treatment accuracy on proton therapy patient selection for oropharyngeal cancer patients.
494 *Radiother Oncol* 2017;125:520–5. <https://doi.org/10.1016/j.radonc.2017.09.028>.
- 495 [32] Kierkels RGJ, den Otter LA, Korevaar EW, Langendijk JA, van der Schaaf A, Knopf AC, et al. An
496 automated, quantitative, and case-specific evaluation of deformable image registration in
497 computed tomography images. *Phys Med Biol* 2018;63:045026.
498 <https://doi.org/10.1088/1361-6560/aa9dc2>.
- 499 [33] Bruijnen T, Stemkens B, Terhaard CHJ, Lagendijk JJW, Raaijmakers CPJ, Tijssen RHN.
500 Intrafraction motion quantification and planning target volume margin determination of
501 head-and-neck tumors using cine magnetic resonance imaging. *Radiother Oncol*
502 2019;130:82–8. <https://doi.org/10.1016/j.radonc.2018.09.015>.
- 503 [34] Cheung JP, Park PC, Court LE, Ronald Zhu X, Kudchadker RJ, Frank SJ, et al. A novel dose-
504 based positioning method for CT image-guided proton therapy. *Med Phys* 2013;40:1–9.
505 <https://doi.org/10.1118/1.4801910>.
- 506 [35] Li B, Lee HC, Duan X, Shen C, Zhou L, Jia X, et al. Comprehensive analysis of proton range
507 uncertainties related to stopping-power-ratio estimation using dual-energy CT imaging. *Phys*
508 *Med Biol* 2017;62:7056–74. <https://doi.org/10.1088/1361-6560/aa7dc9>.
- 509 [36] Wagenaar D, Kierkels RGJ, Free J, Langendijk JA, Both S, Korevaar EW. Composite minimax
510 robust optimization of VMAT improves target coverage and reduces non-target dose in head
511 and neck cancer patients. *Radiother Oncol* 2019;136:71–7.
512 <https://doi.org/10.1016/j.radonc.2019.03.019>.
- 513

514 TABLES AND FIGURES CAPTIONS

515 Table 1 - Study population characteristics (N = 10)

516 * The reported treatment modalities were classified as in the normal-tissue complication probability
517 model for tube-feeding dependence.[15]

518 Table 2 - Average dose of all treatment scenarios including known error distributions for plans 519 created with different robustness setup and range uncertainty criteria (N=10).

520 PC: Pharyngeal constrictor

521 #: For Δ/mm and $\Delta/\%$ the slope of the regression fit is reported

522 *: $p < 0.05$ in a two-tailed paired student t-test.

523 **: $p < \alpha$ after adjusting α using Bonferroni's correction for multiple testing.

524 Figure 1 – Generation of adjusted treatment plans with various uncertainty settings.

525 The following workflow is used to create treatment plans with smaller setup and range uncertainty
526 settings from the clinical plan. The graphs show the dose profile near the targets for the dose
527 distributions generated during the adjusted treatment plan generation. a) First, the clinical dose is
528 calculated as the nominal scenario of the clinically used treatment plan which was robustly
529 optimized with a setup uncertainty setting of 5 mm and range uncertainty setting of 3%. b) Next, a
530 voxel-wise minimum robustness (multi-scenario) evaluation is performed with a shift equal to the
531 difference in robustness setting between the new treatment plan and the clinical treatment plan. In
532 this example, a treatment plan with a 2 mm setup uncertainty setting is created with an identical
533 range uncertainty setting as for the clinically used treatment plan (3%). Therefore, the shift used for
534 the voxel-wise minimum scenarios is 3 mm and 0% range. The resulting dose distribution has the
535 same dose fall-off but is shifted more towards the targets and has a slight underdosage in the target.
536 c) The dose inside the target is overridden to the clinical dose as determined above (step a) to avoid
537 potential underdosage. d) Using voxel-based dose mimicking optimization, a deliverable treatment
538 plan is created with a very similar nominal dose distribution to the predicted dose distribution.

539 Figure 2 - Treatment scenario calculation workflow.

540 To calculate a single treatment scenario the following workflow was followed. To incorporate
541 changes due to changing anatomy, doses were recalculated on the weekly verification CTs. All seven
542 verification CTs were shifted with the same systematic setup and range errors which were sampled
543 from their determined distributions. For each CT, multiple daily fraction errors were sampled from
setup error distribution and applied. Each treatment simulation therefore consists

545 of 35 daily perturbed CTs. This procedure was repeated 25 times for each treatment plan, sampling
546 different systematic and random errors for each treatment scenario.

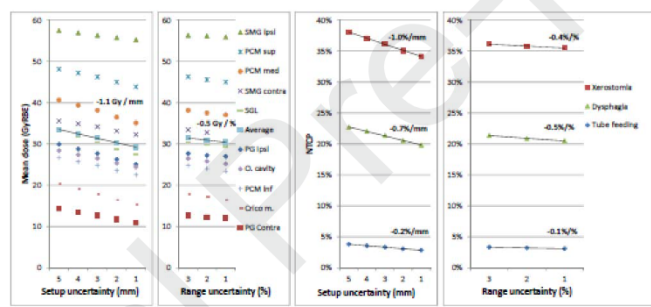
547 **Figure 3 - Simulated clinical target volume dose and tumor control probability as a function of**
548 **robustness setup and range uncertainty**

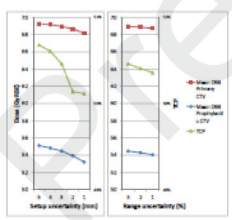
549 The reported doses incorporated known systematic and random setup and range uncertainties and
550 anatomical changes.

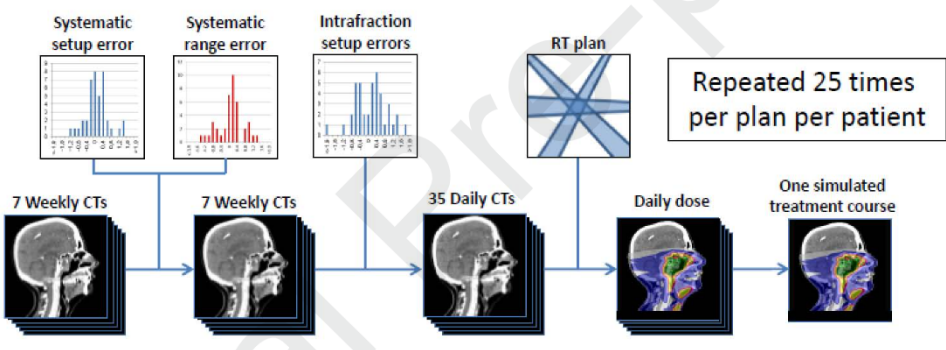
551 **Figure 4 - Simulated organ at risk dose as a function of robustness setup and range uncertainty**

552 The reported doses incorporated known systematic and random setup and range uncertainties and
553 anatomical changes.

554 SMG: Submandibular gland, PG: Parotid gland, ipsi: ipsilateral, contra: contralateral, PCM:
555 Pharyngeal constrictor muscle, SGL: Supraglottic larynx, O. Cavity: Oral Cavity, Crico m.:
556 Cricopharyngeal muscle



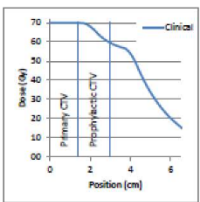
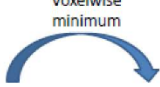




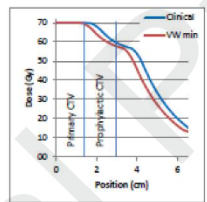
Voxelwise minimum

Overriding target dose

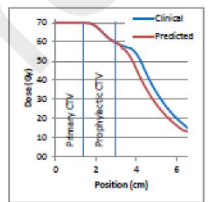
Dose mimicking



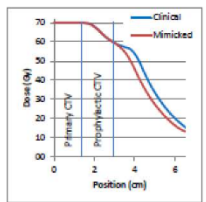
a



b



c



d